DETERMINATION OF OPTIMAL GROUND SAMPLING DISTANCE FOR MATCHING GCP CHIPS AND SATELLITE IMAGES

Y. Lee [1],J. Son[1],T. Kim [2]*

[1]3DLabs Co. Ltd., 1610-ho, 56 Songdogwahak-ro, Yeonsu-gu, Incheon, Korea – (eyoojin2, json8520)@3dlabs.co.kr

[2] Dept. of Geoinformatic Engineering, Inha University, 100 Inharo, Namgu, Incheon, Korea – tezid@inha.ac.kr

Commission I, WG I/8

KEY WORDS: CAS500 Series, GCP Chip Matching, Image Matching, Geometric Correction, Sensor Model, Kompsat-3A, RapidEye.

ABSTRACT:

Many satellites for high resolution image acquisition are being developed very actively worldwide. In Korea, the Government has started a new space program, CAS (Compact Advanced Satellites), to promote image utilization and national space industry. For the successful utilization of satellite images, the geolocation accuracy of them is very important. A research has been performed for automated GCP (Ground Control Point) generation and precise sensor modelling by matching small image chips centered at GCPs against satellite images. In this study, we examined whether GCP chips at 25cm GSD created for CAS-1 images can be used for CAS-4 images at 5m GSD and, if so, whether there is an optimal GSD to improve the matching between GCP chips and CAS-4 images. Due to data availability, experiments were carried out using Kompsat-3A images at GSD of 55cm, as a replacement to CAS-1 image, and RapidEye images at GSD of 5m, as a replacement to CAS-4 images. Original satellite images were upscaled to make test images with various GSDs. GCP chips were downscaled to make their GSD identical to test images. We performed matching with the downscaled GCP chips and the test images. Experiments showed that it was possible to reuse GCP chips at 25cm GSD for satellite images at 5m GSD. When RapidEye images were upscaled to the range of 1.67m GSD (one third of the original GSD) to 1.25m GSD (one fourth), we achieved improved geolocation accuracy then matching GCP chips at the original images (5m GSD).

1. INTRODUCTION

With the increased interest on space industry and New Space Policy, many satellites for high resolution image acquisition are being developed very actively worldwide. In Korea, the Government has started a new space program, CAS (Compact Advanced Satellites), to promote image utilization and national space industry (Kang and Lim, 2015). CAS-1 is the first satellite of the new program with a 500kg medium-sized satellite platform. It was launched in March, 2021, and is capable of capturing panchromatic images at GSD (Ground Sample Distance) of 50cm and multispectral images at GSD of 2m. It twin satellite, CAS-2, will be launched in 2022. CAS-1 and 2 are expected to be used in land monitoring and geospatial information generation (Han et al., 2017; Han et al., 2018). As a follow-on mission, CAS-4 is currently under development with a mission to daily observe Korean Peninsular by multispectral images at FSD of 5m. CAS-4 will be launched in 2025 and used for monitoring crops, agricultural, water resources, and forest resources (Baek and Lee, 2020).

For the successful utilization of satellite images, the geolocation accuracy of them is very important. Many studies have been conducted to improve the geolocation of satellite images (Im et al, 2002; Jeong et al, 2014). In general, one can improve the geolocation accuracy by establishing a precise sensor model with GCPs (Ground Control Points). To generate GCPs for CAS-1 images automatically, research was performed for automated GCP generation and precise sensor modelling (Yoon, 2019; Lee et al., 2020). For each GCP, a small image chip was extracted from nationwide orthoimages at GSD of 25cm generated from aerial images (Park et al, 2020; Lee et al., 2020). A CAS-1 image is matched against GCP chips and matched image locations are used as GCPs for the image.

In this study, we examined whether GCP chips created for CAS-1 images can be used for CAS-4 images and, if so, whether there is an optimal GSD to improve the matching between GCP chips and CAS-4 images. It is notable that while the GSD of GCP chips (25cm) is half of the GSD of CAS-1 panchromatic images (50cm), it is significantly smaller to the GSD of CAS-4 images (5m). Matching images with such different GSDs will be challenging and needs careful investigations.

To this end, we conducted experiments using Kompsat-3A images at GSD of 55cm, as a replacement to CAS-1 image, and RapidEye images at GSD of 5m, as a replacement to CAS-4 images. Firstly, each original satellite images were up-sampled/down-sampled to make test images with various GSDs. Secondly, GCP chips were downscaled to make their GSD identical to test images. We performed matching with the downscaled GCP chips and the test images. For matching, we applied ZNCC(Zero-Mean Normalized Cross Correlation) (Cideciyan et al, 1992; Zheng and Chellapa, 1993) and Census Transform algorithm(Kim et al, 2018). Matched image locations were used as image coordinates for the GCPs used. They were randomly sampled to remove match outliers (Fischler and Bolles, 1981) and used for precise sensor model generation.

Experiments showed that it was possible to reuse GCP chips at GSD of 25cm for satellite images at GSD of 5m. When RapidEye images were upscaled to the range of 1.67m GSD (one third of the original GSD) to 1.25m GSD (one fourth), we achieved improved geolocation accuracy then matching GCP chips at the original images (5m GSD). At all up-sample levels, the achieved geolocation accuracy was from 1.5 to 2 times of the GSD of

* Corresponding author

images tested. When RapidEye images were upscaled to 1m GSD (one fifth) or smaller, the geolocation accuracy was degraded. These results may be originated from the robustness of matching strategy applied (Kim et al, 2018; Park et al, 2020; Lee et al., 2020) or the high radiometric quality of RapidEye images used for tests or both. On the other hands, when Kompsat-3A images were up-sampled to 25cm (half of the original GSD), no accuracy improvement was observed. This result may indicate that since the GSD of the original images was already very close to that of GCP chips, up-sampling did not improve matching performance.

2. DATA

2.1 Data

We used RapidEye images and Kompsat-3A images for experiments. Table 1 shows the characteristics of RapidEye and Kompsat-3A satellites. As mentioned above, RapidEye images had GSD of 5m and Kompsat-3A panchromatic images GSD of 55cm. Red bands of RapidEye images were used for matching. For Kompsat-3A images, pan-sharpening was applied first and pan-sharpened red bands at 55cm GSD were used for matching.

Property	RapidEye	Kompsat-3A
Bit Per Pixel	16 bit	
Band width	Red, Green, Blue, RedEdge, NIR	Pan, Red, Green, Blue, NIR
GSD	5.0m	Pan: 55cm MS: 2.2m
Swath Width	77km	12km

Table 1. Specification of RapidEye and Kompsat-3A images.

Table 2 shows the specifications for GCP chips used. To get precise ground coordinates, we used Unified Control Point database maintained by National Geospatial Information Institute (NGII) of Korea. For image chips, we used national orthoimage database at GSD of 25cm. The size of GCP Chips were 1027 x 1027 pixels, covering roughly 250 x 250m on ground. This database was constructed from aerial images. The orthoimages and GCP chips were color images with red, green, and blue bands. Red bands of GCP chips were used for matching. Figure 1 shows examples of GCP chips. Fine details of surface are captured within the chips.

Ground Coord.	Unified Control Point
Raw Data	Aerial orthoimage
Size	1027 X 1027
GSD	25 cm
Band	Red, Green, Blue

Table 2. Specification of GCP Chips.

Figure 1. Samples of GCP Chips used for experiments.

We prepared RapidEye and Kompsat-3A images over three test areas, Cheonan, Incheon and Yanggu of Korea. Cheonan and Incheon areas contain planar and mountainous regions whereas Yanggu area is covered by mountains mostly. Figure 2 and 3 show RapidEye and Kompsat-3A images, respectively, over the three test areas.

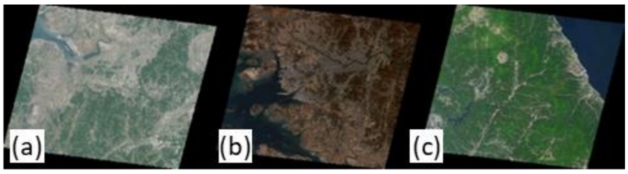

Figure 1. RapidEye images used. (a) Cheonan, (b) Incheon, (c) Yanggu.

Figure 2. Kompsat-3A images used. (a) Cheonan, (b) Incheon, (c) Yanggu.

Table 2 and 3 show specifications of RapidEye and Kompsat-3A images for the three test areas. The number of GCP chips used for each image is also given in the tables.

Area	Cheonan (A)	Incheon (B)	Yanggu (C)
Product	Level 1B		
Acquisition Date	2019.11.07	2019.06.04	2019.05.24
Image Size (Cols X Rows)	11754 X 11965	11824 X 14509	11760 X 14196
Scene Center (Lat, Lon)	39.7074241, 127.4025355	35.2318610, 126.636675	40.387735, 128.7499357
No. of GCP Chips	1304	1828	1603

Table 2. Specification of RapidEye images used.

Area	Cheonan (A)	Incheon (B)	Yanggu (C)
Product	Level 1R		
Acquisition Date	2019.01.29	2018.01.27	2017.04.29
Size (Cols X Rows)	24060 X 24400	24060 X 18800	24060 X 19680
Scene Center (Lat, Lon)	36.8331488, 127.1324747	37.47981407 126.6632889	38.1201508, 127.9349215

No. of GCP Chips	40	49	62

Table 3. Specification of Kompsat-3A images used.

3. METHOD

3.1 Method

The method applied in this paper was performed according to Figure 4. The following description of each step is shown. First, each original satellite images were upscaled by difference factors to make various test images at smaller GSDs. In case of RapidEye images, we upscaled the original images by 2, 3, 4, 5, 6, and 7 times. These up-sampling scales correspond to GSD of 2.5m, 1.67m, 1.25m, 1m, 83cm and 71cm. For Kompsat-3A images, we up-sampled the original images at 50cm GSD by 2 times (25cm GSD).

For each up-sampled image, we converted RPCs (Rational Polynomial Coefficients) for original images by applying new offsets and scales for up-sampled images. When up-sampling factor is r, new offsets and scales ($Col'_{Offset}, Row'_{Offset}, Col'_{Scale}, Row'_{Scale}$) are calculated from original offsets and scales as Ep. 1 to 4.

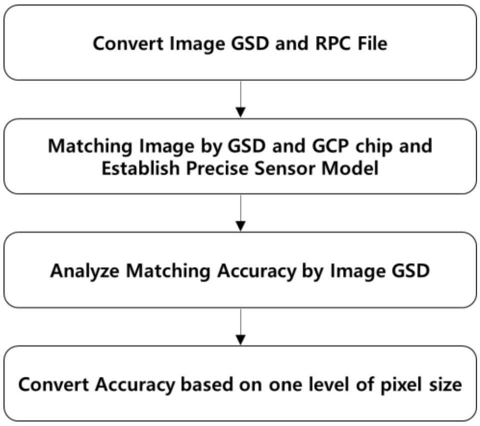

Figure 3. Flow Chart of Experiment.

$$Col'_{Offset} = r \times Col_{Offset} \quad (1)$$

$$Col'_{Scale} = r \times Col_{Scale} \quad (2)$$

$$Row'_{Offset} = r \times Row_{Offset} \quad (3)$$

$$Row'_{Scale} = r \times Row_{Scale} \quad (4)$$

Secondly, GCP chips were downscaled to make their GSD identical to test images. For examples, they were downscaled by the factor of 20 to make their GSD as 5m and matched against the original RapidEye images at 5m GSD. They were downscaled by the factor of 10, 6.7, 5, 4, 3.3, 2.9 and 2 to make their GSD equivalent to 2.5m, 1.67m, 1.25m, 1m, 83cm, 71cm and 50cm. The down-sampled GCP chips were matched against their corresponding up-sampled or original images at the same GSD. For matching, the following procedure in Figure 5 was applied.

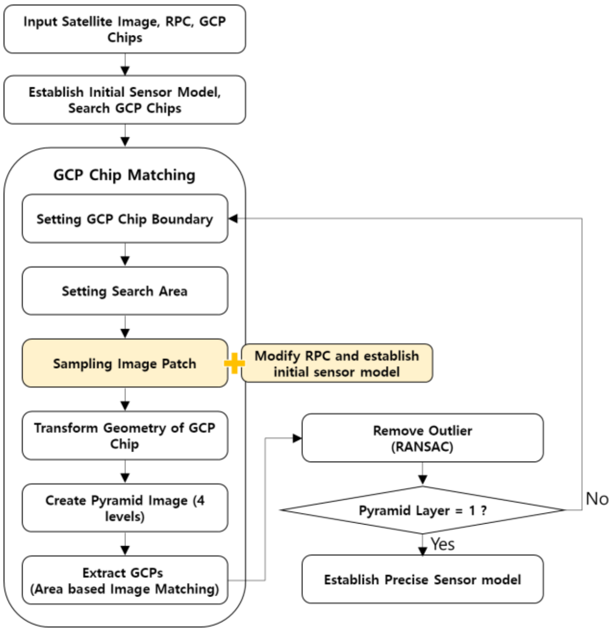

Figure 4. Flow of GCP Chip matching algorithm.

After inputting an original or up-sampled satellite image, an original or modified RPC file and down-sampled GCP chips, we established an initial sensor model with the input RPC file. We calculated image locations of the GCP chips using the initial sensor model and defined search areas. We resampled the downscaled GCP chips again according to image geometry using the initial sensor model. Matching was performed at 4-layer pyramid. ZNCC was applied to the top three layers and Census algorithm to the last layer. For each layer, we applied RANSAC (Random Sample Consensus) algorithm to remove outliers. Inliers at earlier layer were passed to the next layer and used as the initial image location of GCP chips.

Next, GCPs generated automatically through matching were used for establishing a precise sensor model. The accuracy of precise sensor models was estimated by the accuracy of model points and by the accuracy of independent check points. We measured check points manually to be distributed uniformly within image space.

Finally, precise sensor models established at up-sampled scales were converted back to the original image scale and their accuracy was analyzed in meters.

4. EXPERIMENTS

4.1 Matching results for RapidEye Images

Table 5 shows the results of experiments with RapidEye images. We measured initial sensor model accuracy (I_Acc) and precise sensor model accuracy (M_Acc) in pixels for each test image. The percentage of successfully matched GCP chips (Inlier Rate) was also checked. The accuracy of precise sensor models was measured by the accuracy of model points (OM_Acc) and the accuracy of check points (OC_Acc). Check point accuracy for the three areas was averaged to indicate the performance of geolocation accuracy at an up-sample scale (OC_Avg).

Image GSD (m)	Area	I_Acc (pixel)	M_Acc (pixel)	Inlier Rate (%)	OM_ Acc (m)	OC_ Acc (m)	OC_ Avg (m)
5.0	A	2.423	1.271	65%	6.355	**7.042**	**7.748**
	B	2.679	1.303	64%	5.320	**9.222**	

	C	2.179	1.382	57%	6.937	**7.218**	
2.5	A	2.654	1.217	82%	3.047	**2.242**	**3.186**
	B	2.948	1.245	85%	3.458	**3.847**	
	C	2.341	1.256	85%	3.488	**3.372**	
1.67	A	3.551	1.033	88%	1.722	**1.843**	**2.782**
	B	3.866	0.952	86%	1.585	**3.662**	
	C	2.763	0.919	94%	1.525	**2.778**	
1.25	A	4.397	0.967	83%	1.192	**1.400**	**2.734**
	B	4.932	0.959	94%	1.198	**4.721**	
	C	3.969	0.821	90%	1.025	**3.213**	
1.0	A	5.837	1.032	92%	2.867	**3.603**	**3.635**
	B	5.602	0.974	91%	0.975	**5.720**	
	C	4.713	0.933	88%	2.600	**4.763**	
0.83	A	6.05	0.983	85%	0.820	**2.082**	**2.87**
	B	6.201	0.974	91%	0.810	**3.255**	
	C	5.047	0.983	93%	0.820	**3.162**	
0.71	A	6.128	0.985	93%	0.703	**2.330**	**2.936**
	B	5.909	0.975	83%	0.697	**3.072**	
	C	5.289	0.974	92%	0.697	**3.543**	

Table 4. Measurement of GCP Chip matching performance of RapidEye image by GSD

Table 5 shows that initial sensor model accuracies in pixel (I_Acc) were proportionally increased as GSD of test images became smaller. This result is natural since initial sensor models for each test area are identical and differ only by the factor of up-sample scales. Matching was applied and precise sensor models were established. The model accuracy of precise sensor models in pixels (M_Acc) and the inlier rate show that GCP chip matching was applied successfully at all image GSDs. It is interesting to see that model errors were around one pixel in all cases. This indicates the level of precision of matching algorithm applied for experiments.

Figure 3 and 4 show the results of successfully matched GCP chips and outliers. Backward image is satellite image, and small image is GCP Chip. And the red box is matching point calculated result of GCP Chip matching. In figure 3, it shows that GCP Chip best fit to geographic features around it. On the contrary, in figure 4, it shows that GCP Chip does not fit to geographic features around it.

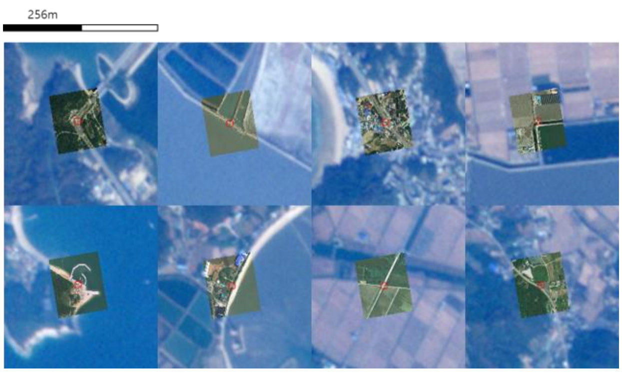

Figure 5. GCP Chips that matched as inlier.

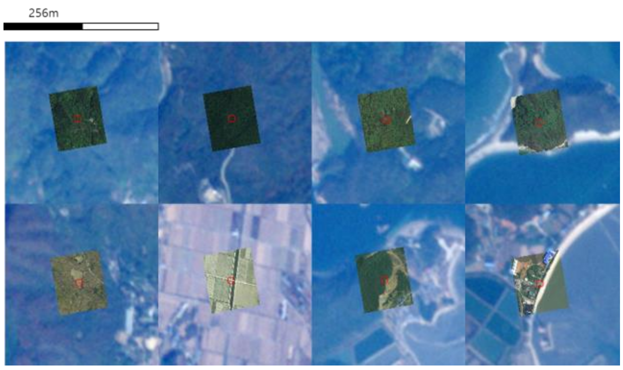

Figure 6. GCP Chips that matched as outlier.

OM_Acc in Table 5 is calculated by applying GSDs to M_Acc for each case. The modelling accuracies in meters seem continuously improved as the image GSD get smaller. However, when we used independent check points for accuracy analysis (OC_Acc and AC_Avg), the images with GSD of 1.67m and 1.25m showed best accuracy. Figure 5 to 7 show the result of GCP chip matching performance by image GSD. In the table, area A is Cheonan, B is Incheon, and C is Yanggu.

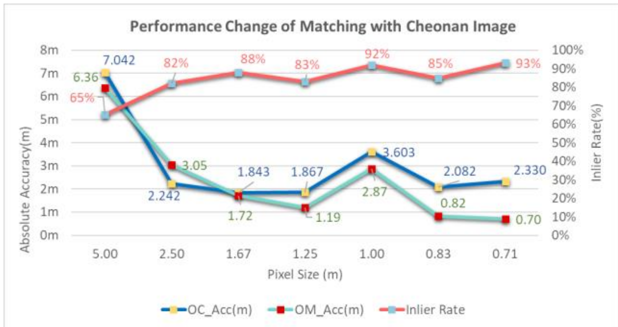

Figure 7. Performance change of matching with Cheonan RapidEye image.

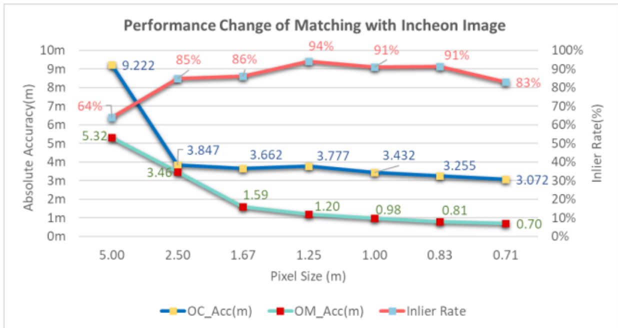

Figure 8. Performance change of matching with Incheon RapidEye image.

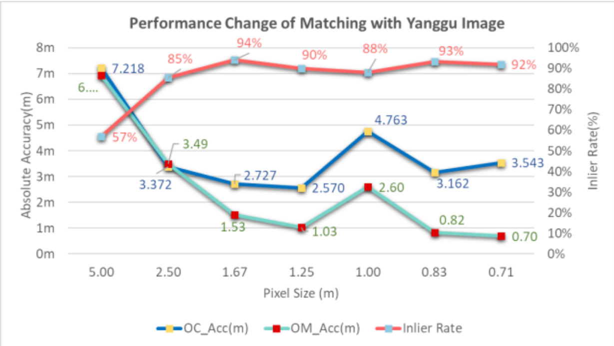

Figure 9. Performance change of matching with Yanggu RapidEye image.

As we can see in Table 5 and Figures 5 to 7, we could apply matching to GCP chips developed for CAS-1 images (50cm GSD) to RapidEye images (5m GSD). Moreover, we could achieve improved geolocation accuracy by upscaled the original images at 5m GSD to smaller GSDs of 1.25m to 1.67m. This corresponds to upscaled the original image by three to four times. We can also observe that Incheon and Yanggu's precise sensor model accuracy (OC_Acc) were worse about 1 ~ 2m than Cheonan due to its coverage of mountain and sea was high.

4.2 Matching results for Kompsat-3A Images

GCP chip matching was also applied to Kompsat-3A images. Table 6 shows the results of experiments with Kompsat-3A images. For Kompsat-3A images, the original images at 50cm GSD were up-sampled by the factor of two and the images at 25cm GSD was created. The original images were downscaled by the factor of three (1.5m GSD) for additional accuracy check.

Initial and precise sensor model accuracies were analyzed as before. Table 6 and Figures 8 to 10 show the result of measuring GCP Chip matching performance by various image GSDs.

Image GSD (m)	Area	I_Acc	M_Acc	Inlier Rate (%)	OM_ Acc (m)	OC_ Acc (m)	OC_ Avg (m)
1.5	A	1.335	1.063	60%	0.532	**2.504**	**3.173**
	B	7.342	1.224	37%	0.612	**4.407**	
	C	3.914	0.987	24%	0.494	**3.572**	
0.5	A	2.477	1.744	93%	0.872	**1.059**	**1.254**
	B	18.603	1.265	61%	0.633	**1.004**	
	C	6.133	1.380	55%	0.690	**1.656**	
0.25	A	3.701	1.194	95%	0.298	**0.980**	**1.642**
	B	40.184	1.246	82%	0.306	**1.845**	
	C	22.171	1.361	77%	0.341	**2.445**	

Table 5. Measurement of GCP Chip matching performance of Kompsat-3A image by GSD.

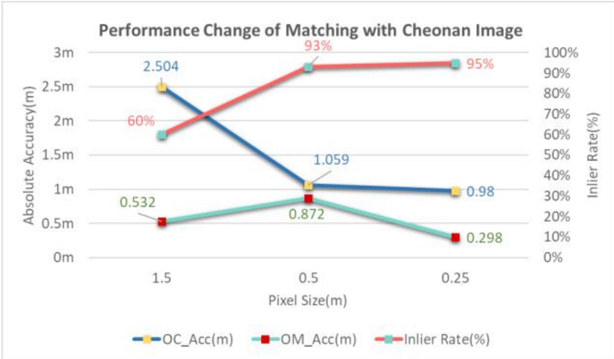

Figure 10. Performance change of matching with Cheonan Kompsat-3A image.

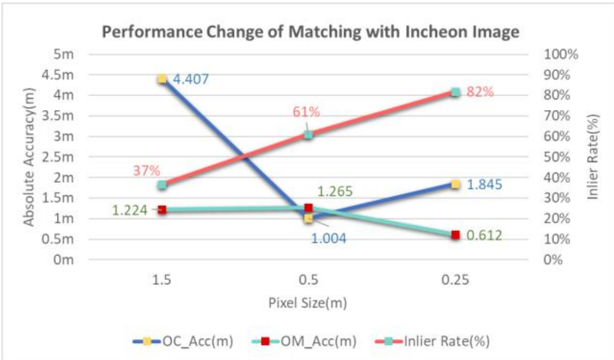

Figure 11. Performance change of matching with Incheon Kompsat-3A image.

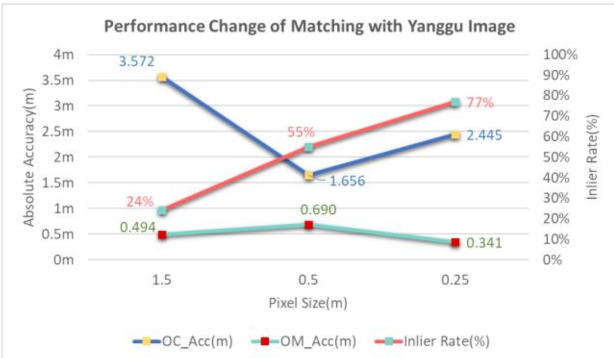

Figure 12. Performance change of matching with Yanggu Kompsat-3A image.

As we can see in Table 6, model accuracies were improved with smaller image GSD. However, the best check accuracy was when the matching was applied to the original images. Since the GSD of Kompsat-3A images was two times of that of GCP chips, up-sampling by the factor of two did not improve the accuracy of sensor models.

CONCLUSION

As a result of analyzing performance of GCP chip matching at various image GSDs, it was found that in case of RapidEye images tested, images at GSD of 1.25m to 1.67m showed the best accuracy and in case of Kompsat-3A images, images at GSD of 0.5m. We can conclude that it is possible to reuse GCP chips at 25cm GSD for matching against satellite images at 5m GSD and hence for CAS-4 images. This positive conclusion may support the robustness of matching strategy applied. When RapidEye images were upscaled to the range of 1.67m GSD (one third of the original GSD) to 1.25m GSD (one fourth), we achieved improved geolocation accuracy then matching GCP chips at the original images (5m GSD). These results may be originated from the robustness of matching strategy applied or the high radiometric quality of RapidEye images used for tests or both. We may expect accuracy improvement for up-sampled CAS-4 images. However, the level of improvement and optimal up-sampling levels are yet to be researched further.

We also found that excessive up-sampling was not helpful for matching performance. Indeed, Kompsat-3A, which already has similar GSD to that of GCP chips, original images showed the best matching performance. In the future, we need to study on improving matching performance of CAS-1 images by using other up-sampling factors and by preparing high-quality GCP chips.

ACKNOWLEDGEMNETS

This research was supported by a grant of “Development of marine satellite image analysis application technology (20210046)” funded by the Korea Hydographic and Oceanographic Agency.

REFERENCE

Kang, M. and Y, Lim., 2015. A study on the application demand of satellite-based information to support national land polices, *Korea Research Institute for Human Settlements*, 1-124 (in Korean with English abstract).

Baek, M.J and Lee, S.G, 2020. Introduction of the Development of CAS500-4 EO Payload with Wide Swath, *The Korean Society for Aeronautical and Space Sciences*, 1-2.

Han, C.Y., Kim, J., and Kim, S.S., 2017. Optimised Design of Standard Platform for CAS500 satellite, *The Society for Aerospace System Engineering*, 219-220.

Lee, Y.J., Park, H.J., Kim, H.S. and Kim, T.J., 2020. Analysis of Geolocation Accuracy of Precision Image Processing System developed for CAS-500, *Korean Journal of Remote Sensing*, 36(5-2): 893-906 (in Korean with English abstract).

Im, Y., Kim, T.J., and Kim, J., 2002. DEM Extraction from KOMPSAT-1 EOC Stereo Images and Accuracy Assessment, *Korean Journal of Remote Sensing*, 18(2): 81-90 (in Korean with English abstract).

Jeong, J.H., Kim, J., and Kim, T.J., 2014. Analysis of Geolocation Accuracy of KOMPSAT-3 Imagery, *Korean Journal of Remote Sensing*, 30(1): 37-45 (in Korean with English abstract).

Yoon, W.S., 2019. A Study on Development of Automatic GCP Matching Technology for CAS-500 Imagery, *Inha University*, Incheon, Korea (in Korean with English abstract).

Park, H.J., Son, J.H., Jung, H.S., Kweon, K.E., Lee, K.D., and Kim, T.J., 2020. Development of the Precision Image Processing System for CAS-500, *Korean Journal of Remote Sensing*, 36(5): 881-891 (in Korean with English abstract).

Kim, J.I. and Kim, H.C. 2018. Performance Comparison of Matching Cost Functions for High-Quality Sea-Ice Surface Model Generation, *Korean Journal of Remote Sensing*, 34(6-2): 1251-1260 (in Korean with English abstract).

Fischler, M. A. and R.C. Bolles, 1981. Random sample consensus: a paradigm for model fitting with applications to image analysis and automated cartography, *Communications of the ACM*, 24(6): 381-395.

Cideciyan, A.V., S.G. Jacobson, C.M. Kemp, R.W. Knighton, and J.H. Nagel, 1992. Registration of high resolution images of the retina, *Proc. SPIE 1652, Medical Imaging VI: Image Processing*, 1652:310-322.

Zheng, Q. and R. Chellappa, 1993. A computational vision approach to image registration, *IEEE Transactions on Image Processing*, 2(3):311-326.

Han, C.Y., Kim, J., and Kim, S.S., 2018. Trade-off Study of Mechanical Design for CAS500 satellite, *The Society for Aerospace System Engineering*, 252-253.